Thermal Rejuvenation of the Yermak Plateau

NILGÜN OKAY[1,2] and KATHLEEN CRANE[1,2,3]

[1]*Department of Earth and Environmental Sciences, The Graduate School and University Center of City University of New York, 33 West 42nd Street, New York, NY 10036, U.S.A.*
[2]*Department of Geology and Geography, Hunter College of City University of New York, 695 Park Avenue, New York, NY 10021, U.S.A.*
[3]*Lamont-Doherty Earth Observatory, Palisades, NY 10694, U.S.A.*

Abstract. The Yermak Plateau, bordering the Arctic Ocean and the Norwegian-Greenland Sea, and adjacent to the continental Svalbard Archipelago, is characterized by high heat flow relative to its surrounding region. South of and parallel to the trend of the plateau lies the formerly active-Spitsbergen Shear Zone (De Geer Zone), which is now occupied by the slowly spreading Knipovich and Molloy Ridges. An analysis of these heat flow data suggest that asymmetric spreading within the Norwegian-Greenland Sea propagated northwards along one of the faults associated with the Spitsbergen Shear Zone. The broad zone of faults, once associated with this paleo-shear zone, extends throughout Svalbard as well as on and to the west of the Knipovich Ridge. This network of faults may comprise a complex system of detachment surfaces along which magma may rise from a deep-seated source and across which simple shear extension may develop. Dike injection into the Yermak Plateau, north of the propagating ridge may have been initiated by the thermal response of the highly fractured lithosphere to this propagating asthenospheric front. We suggest that one of these faults, acting as a secondary detachment to the main fault underlying the Knipovich Ridge, may be dissecting the Yermak Plateau. Based on an analysis of the thermal data, simple shear extension may have been taking place along a broad zone of intrusion. This region has undergone and is probably still undergoing thermal rejuvenation. Multiple zones of intrusion may be a common phenomena along newly rifted continental margins especially when they have been substantially faulted prior to rifting.

Introduction

It has been proposed that during the breakup of a continent, a rift zone propagates from its point of initiation of maximum state of stress to the area which is under a reduced state of stress (Bonatti and Crane, 1982; Crane and Bonatti, 1987). Pre-existing faults and other zones of crustal weakness may severely impede the path that a propagating rift would take under homogeneous conditions by abruptly lowering the state of stress into which the rift may propagate. Thus, when a propagating rift tip encounters a pre-existing fault it is likely to change its direction of motion to coincide with the trend of the crustal weakness-zone.

Where a propagating asthenospheric tongue intersects a pre-existing fault zone, magma may erupt rapidly to the surface along the faults if they cut deeply enough through the crust. In this manner pre-existing faults may completely or partially trap the propagating asthenospheric tongue. Should the fractures in the crust be decoupled from the asthenosphere then the deep seated portion of the propagating tongue may proceed in the direction it was moving, depending on the state of stress at depth. This could lead to the situation where underplating and heating of the continental lithosphere occurs in places far removed from the fault controlled surface extrusion of magma. It follows that the surface expression of the new 'plate boundary' may evolve along the axis of one of the pre-existing faults while the subjacent asthenospheric tongue continues to move in its pre-ordained direction (Crane et al., 1988, 1991).

Intrusion by dikes into the crust located ahead of the surface expression of a propagating rift tip may be one mechanism by which continents become underplated and weakened by mantle material (Bonatti, 1985). The forward end of the propagating asthenospheric tongue would be submerged deeply below continental crust while the 'aft' portion would be close to the surface resulting in accretion of oceanic crust. Evidence for the deep-seated 'forward' portion of an asthenospheric tongue may be documented by: (1) observing a large thermal swell on the continent ahead of the propagating rift, (2) observing very large erosion and sedimentation rates in-

dicative of rapid uplift, and (3) sampling oceanic type mantle rocks at shallow levels on the edges of a continental margin.

Multiple zones of magma entrapment may occur within any number of pre-existing faults associated with a paleo-shear zone. Should the deep seated asthenospheric tongue continue to propagate in its original direction, successive episodes of extrusion could occur as one pre-existing fault at a time is crossed. The net effect on the surface would be the appearance of multiple parallel zones of extrusion creating a broad-diffuse plate boundary.

Complicating this entrapment model is the role of changing stress fields due to the reorientation of the propagating rift. Assuming that surface extension occurs at right angles to the direction of propagation, when the propagating rift tip hits a formerly active shear zone, the crust within the acute angle side of impact will be subjected to compression and the crust on the obtuse angle side will continue to be subjected to extension (Crane et al., 1988). These asymmetric stresses concentrated in the upper crust may contribute to the evolution of an asymmetrically spreading ridge.

Additional complications in the spreading geometry may arise in response to the magnitude and dip of the paleo-shear zones which trapped the propagating rift. Should the paleo-shear zone be constructed of steeply dipping faults they may act as detachment surfaces across which new crust is accreted (Wernicke, 1985; Lister et al., 1986; Buck et al., 1988). Rifting across a detachment fault may also generate extreme extensional asymmetry forcing the spreading center to remain on one side of the newly developing ocean basin (Buck et al., 1988; Martínez et al., 1988; Crane et al., 1991).

All of the discussions gain an air of authenticity when we look at actual cases where both young, propagating rifts and their interactions with pre-existing fault zones are observed (Bonatti and Crane,

1982; Bonatti, 1985; Crane and Bonatti, 1987). This scenario appears to have happened in the earliest history of the equatorial Atlantic (Bonatti and Crane, 1982) which opened along a broad feature: the Equatorial Megashear Zone. In the Red Sea, a youthful propagating rift may be impinging obliquely upon a series of shear zones parallel to the Dead Sea Fault (Courtillot, 1982; Bonatti and Crane, 1982, 1984; Crane et al., 1988). A classic example of a propagating rift located in a paleo-shear zone can also be found in the Norwegian-Greenland Sea (Talwani and Eldholm, 1977; Vogt et al., 1981; Myhre and Eldholm, 1988; Crane et al., 1988, 1991; Okay, 1990; Okay and Crane, 1991) (Figure 1). Here the NE trending Mohns Ridge has entered the Spitsbergen Shear Zone (also called De Geer Zone), and has formed the northward trending Knipovich Ridge, among the slowest spreading centers in the world. Rifting and spreading across the paleo-shear zone has led to the extremely oblique and asymmetric opening about the Knipovich Ridge. Directly to the north of the tip of the Knipovich Ridge lies the Yermak Plateau which parallels the trend of the small offset Molloy and Spitsbergen Transform Faults. This plateau has undergone recent heating and is thus an enigmatic feature – not clearly continental nor oceanic in its provenance. Its transitional state may provide clues to the rates and styles of rifting in transitional areas (Dietz and Shumway, 1961; Johnson, 1975; Talwani and Eldholm, 1977; Vogt et al., 1981; Crane et al., 1982; Jackson et al., 1984; Myhre and Eldholm, 1988) (Figures 1 and 2).

Genesis and Morphotectonic Setting

The Yermak Plateau was first interpreted as a downfaulted portion of the continental margin (Johnson, 1975). However, a downfaulted continental fragment is difficult to accommodate when plate reconstructions are considered in this area. Jackson et al.

Fig. 1(a). Simplified models showing the tectonic evolution of the region adjacent to the Yermak Plateau, the movement of three plates (Anomaly 24), GR: Greenland, NA: North America, EU: Eurasia. Bathymetry is indicated by 2000 m contour (after Jackson et al., 1984). (b) The relative motion between Greenland and Svalbard was dominated by strike-slip movement until Anomaly 13 (ca. 35.9 Ma), subsequently followed by seafloor-spreading. Using pole rotation for the Eurasian plate relative to the Greenland plate (after Srivastava and Roest, 1989). Hatched area marks gaps (dominated by extension) between continental margins; stippled areas mark overlaps; dark area marks compression-transpression. The opening of the Norwegian Sea (along the Knipovich Ridge) and the Eurasian Basin along the Nansen Ridge (NR) started along the western margin of Svalbard, giving rise to an extensional tectonic regime. The location of Svalbard relative to the Yermak Plateau (Y), across the Nansen Ridge is a similar feature, the Morris Jesup Rise (M). NW-SE trending faults are shown in dashed lines; Hornsund Fault (hf): (c) Magnetic anomalies of the Yermak Plateau. High-amplitude, low wavelength magnetic anomalies are superimposed on the bathymetric 1500 m contour (after Feden et al., 1979).

A
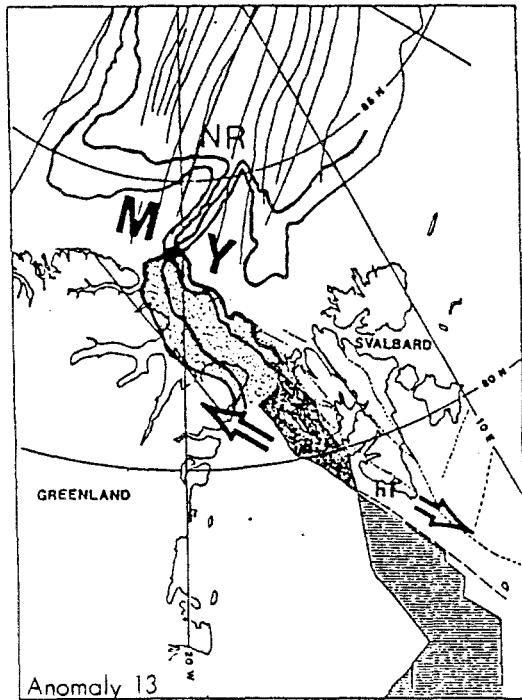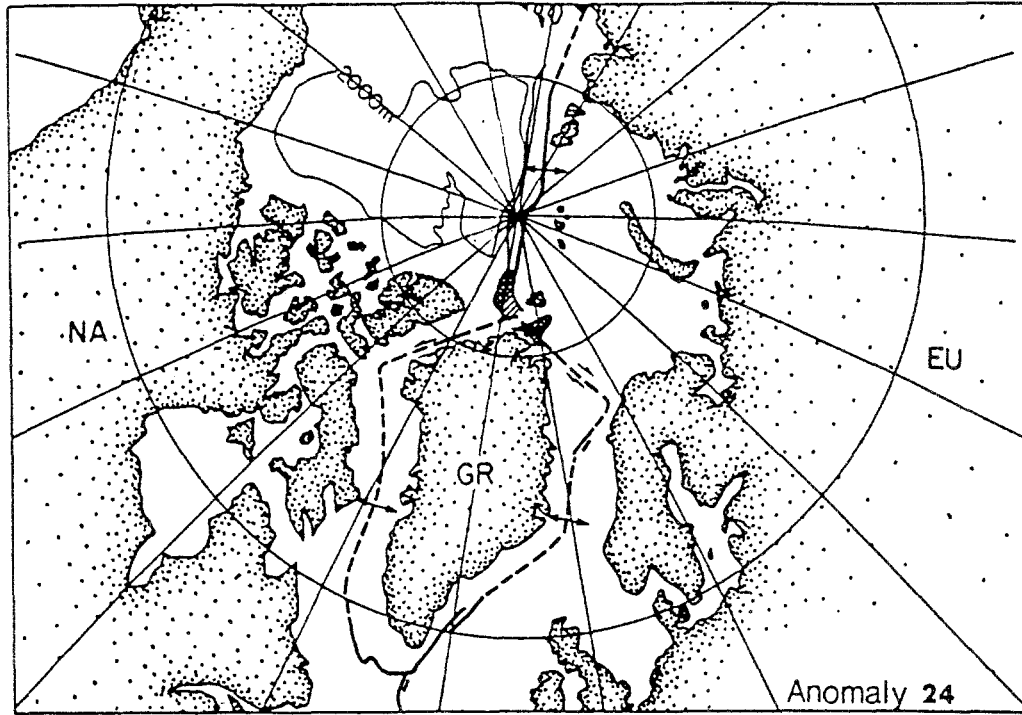
B
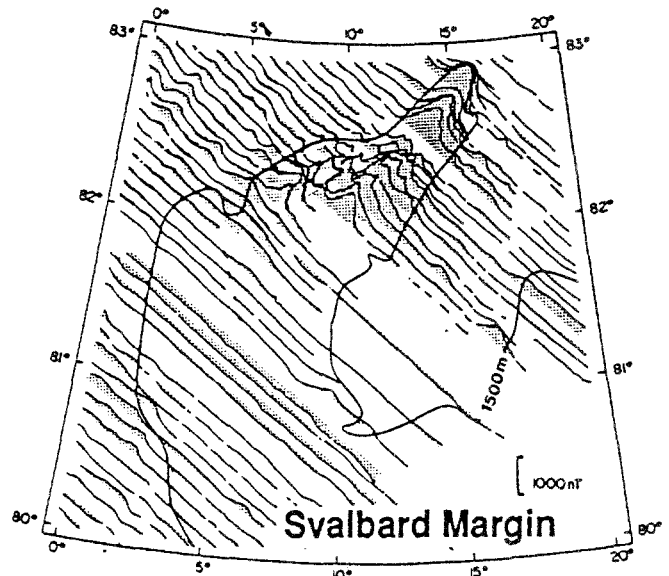
C

Fig. 1.

(1984), using seismic refraction, gravity results and additional heat flow data collected from ice stations, concluded that the plateau could be divided into two different geological parts. The history of the northern part of the plateau has been influenced by seafloor spreading at the Nansen Ridge, the Arctic extension of the Mid-Atlantic Ridge. An analysis of magnetic anomalies in this region suggests that the northern part was formed as oceanic crust from the period between anomalies 24 to 13. During this time three plates were in motion (Talwani and Eldholm, 1977); North America, Greenland and Eurasia (Figure 1a). It is possible that this northern section of the Yermak Plateau formed as a hot spot in conjunction with the Morris Jesup Rise off of Greenland (Figures 1a and 1b). As a consequence of massive basalt outpourings at the triple junction, the Morris Jesup Rise and part of the Yermak Plateau formed a continuous Iceland-like massif. After anomaly 13 ($\sim$ 36 Ma), when Greenland ceased to move relative to North America, and only North America and Eurasia were in motion, the triple junction to the north of Greenland became extinct, isolating and separating the Yermak Plateau from the Morris Jesup Rise (Srivastava and Roest, 1989; Müller and Spielhagen, 1990) (Figure 1b). The southern part of the plateau may have been formed by the thinning and stretching and later dike intrusion of continental crust. Jackson et al. (1984) also cited that rocks dredged from the top of the plateau were gneissic. As many rocks of this composition and metamorphic grade are found in the Hecla Hoek complex of northern Spitsbergen (Winsnes, 1965). Jackson et al. (1984) interpreted the crustal makeup of the southern part of the plateau to also be of the Hecla Hoek formation. However, no fresh surfaces were found on the samples and thus they may have been glacially rafted debris.

Prior to anomaly 13, the Hornsund Fault (once a part of the Spitsbergen Shear Zone and now located on the western margin of Svalbard), together with similar faults on Svalbard, acted as a regional zone of translation between the Greenland and the Eurasian Plates. According to Crane et al. (1988) seafloor spreading was not initiated adjacent to Svalbard until 40 Ma having propagated from the Mohns Ridge in the south to its present day intersection with the Molloy Transform Fault. Because transtension and transpression must have developed over what was once a translational plate boundary after the Greenland plate became fixed in place (Müller and Spielhagen, 1990), much of western Spitsbergen was subjected to episodes of uplift, extension and shear, highly deforming the new continental margin.

Under the effects of elevated regional deviatoric stress the rift propagated northwards. Continued propagation of the Knipovich Ridge at 15 Ma may have cut off the more southerly Hovgård Ridge (now a 'fossil ridge') from its original continental provenance (Crane et al., 1988, 1991). The propagation event coincided with an episode of increasing spreading rates and the thermal rejuvenation of the crust to the north of the Hovgård Ridge as marked by the distinctly different heat flow profiles both north and south of the ridge. At the present time, the tip of the northwards propagating Knipovich Ridge lies directly to the south of the Yermak Plateau (Crane et al., 1988, 1991) where it intersects the Molloy Transform Fault (Figure 2). Structural data interpreted from recently collected SeaMARC II side-looking sonar images (Sundvor et al., 1991; Okay et al., 1991) suggest that block faulting related to extension is occurring on the southern Yermak Plateau margin, north of the intersection of the Knipovich Ridge with the Molloy Transform Fault.

To the north and northwest, the plateau is bordered by the Barents abyssal plain. To the west, the flank of the Nansen Ridge (see Figure 1a) abuts the plateau. This section of the plateau is flat-topped and trends about 150 km in a northeast-southwest direction, narrowing to the northeast (Sundvor et al., 1982a, 1982b). The entire crest of the northern part of the plateau coincides with high amplitude, long wavelength magnetic anomalies (Feden et al., 1979; Okay et al., 1991) (Figure 1c). The high degree of magnetization of the crust in the north differs substantially from the rather subdued magnetic signature associated with the southern part of the plateau (Jackson et al., 1984). On this section of the plateau Crane et al. (1982) measured high heat flow where the seismic signature was consistent with oceanic-type crust (Amundsen et al., 1988).

The eastern flank of the Yermak Plateau is rough and blocky (Sundvor et al., 1982b). Several well defined normal faults at approximately 16°30′ E are aligned parallel to the Widjefjord fault zone located to the south on Svalbard. Recently collected SeaMARC II
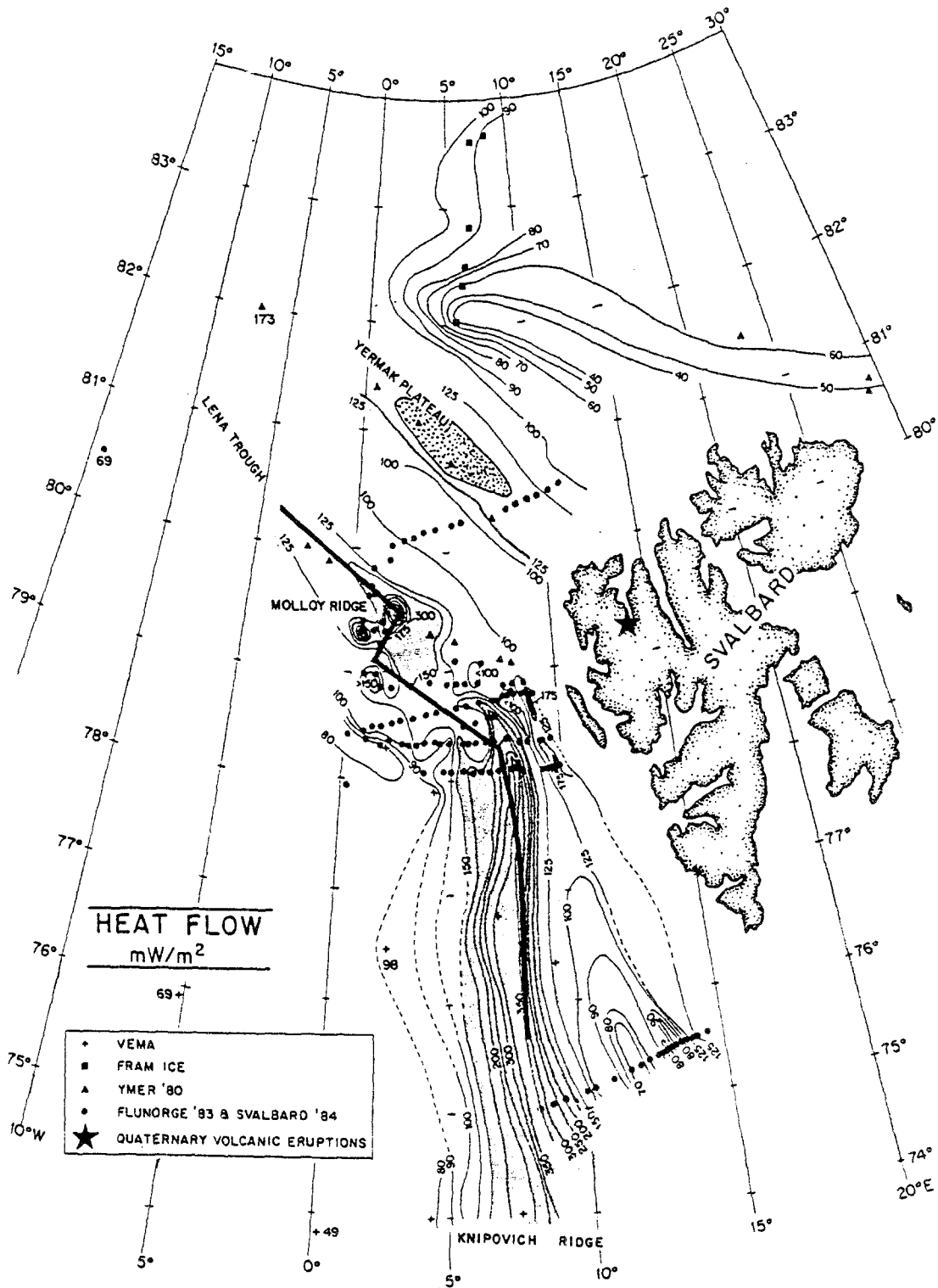
Fig. 2. Heat flow data and simplified plate boundaries within the Norwegian-Greenland Sea. The northern Norwegian-Greenland Sea basin adjacent to Svalbard, Knipovich Ridge, Molloy Ridge and the Yermak Plateau yield relatively high heat flow values (>138 mW m^{-2}) collected by Crane *et al.* (1988, 1991) on Flunorge (1983), Svalbard (1984), and YMER (1980).

data suggest that the NW-SE trending faults border-
ing this eastern flank of the Yermak Plateau may be
the loci of off-axial volcanic eruptions (Okay et al.,
1991). Two strips of acoustically highly reflective and
highly magnetic seafloor (amplitudes > 350 nT) were
detected north of Svalbard as far east as 29° E. These

regions are presumed to be extensions of subaerial
fissure/fault controlled plateau basalts located on the
margins of Nordaustlandet.

A major submarine canyon (Sundvor et al., 1982a)
is incised deeply into the eastern flank of the plateau
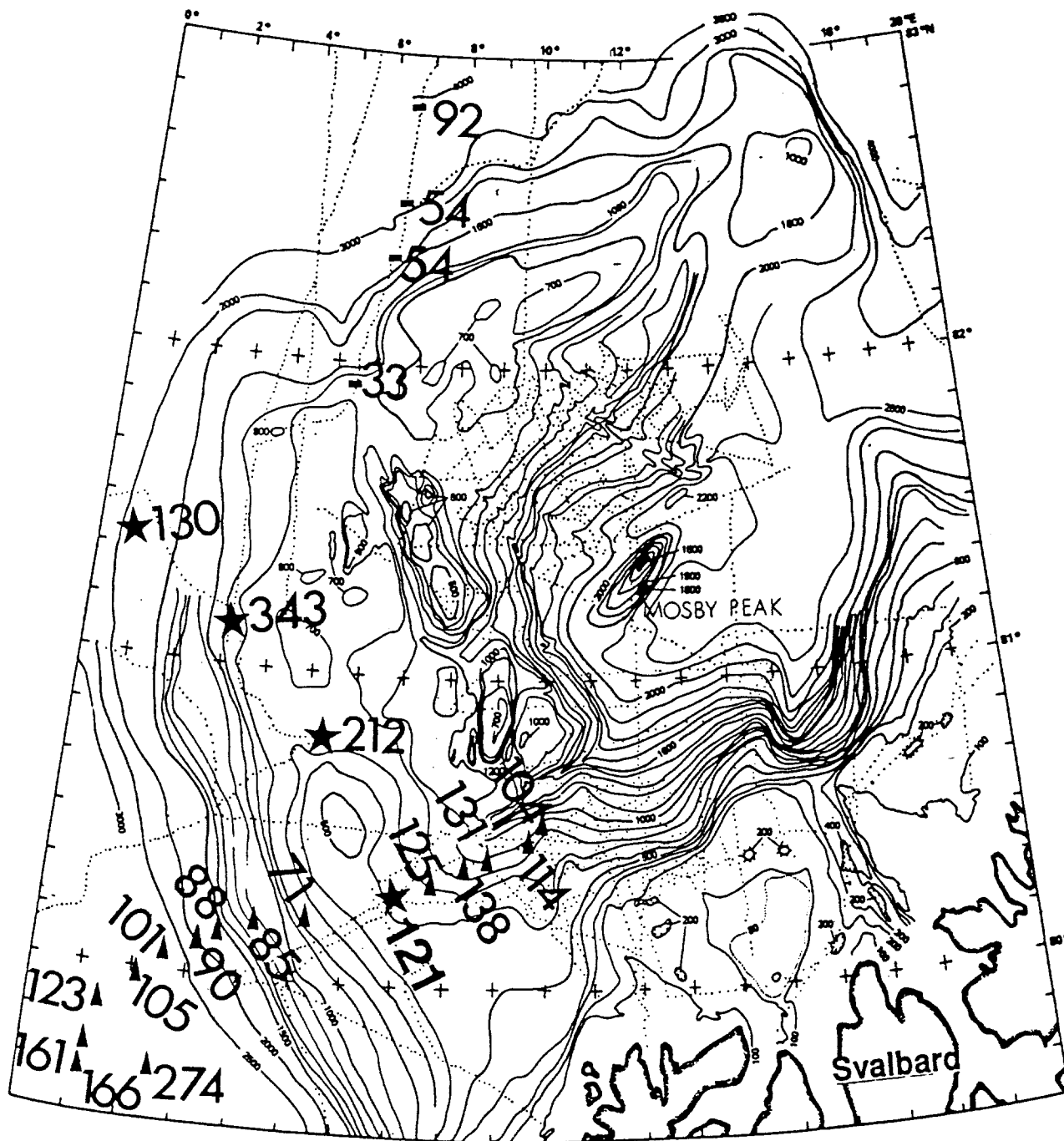(Figure 3). It drains into the Arctic Ocean abyssal

Fig. 3. Bathymetry (Jackson et al., 1984) and heat flow data on the Yermak Plateau Crane et al. (1982) (stars), Jackson et al. (1984)
(dashes), and Sundvor (1986) (triangles). Note Mosby Peak marked by a distinct magnetic anomaly, 250 nT (Okay et al., 1991). Dotted
lines indicate seismic profiles collected by Sundvor et al. (1982).

plain and serves as a major conduit for sediment transport along both the northwestern Svalbard margin and the southeastern Yermak Plateau. The SeaMARC II bathymetric data suggest that the canyon reaches a depth of 2200 m (Okay *et al.*, 1991) along the extreme northern side of the eastern flank. The canyon floor is rather lumpy which may reflect slumps from the adjacent walls. The sediments covering the crest of the canyon walls are irregular in relief, reflecting bottom current activity. The presence of strong bottom currents in this region is to be expected since Atlantic water flows north and east into the Arctic forming erosional channels (Sundvor *et al.*, 1982b).

An extension of the Hornsund Fault Zone (Sundvor *et al.*, 1978) lies along the western edge of the

plateau (Figure 4). Unlike the eastern flank, the western flank deepens rapidly to more than 4000 m culminating in the Spitsbergen Transform Fault (Birkenmajer, 1981; Thiede *et al.*, 1990).

The southern section of the plateau extends to approximately 81°15′ N. The flank of the plateau in this region trends north-northwest and is enclosed by the 700 m isobath shoaling to 490–570 m on two structural benches (Sundvor *et al.*, 1982a, 1982b; Okay *et al.*, 1991) (Figure 3). Sundvor *et al.* (1979) suggested that the southern part of the plateau was formed or at least modified by the extrusion of oceanic basalts overprinting highly faulted and extended continental crust. Their interpretations were based on the seismic velocity structure of acoustic basement and the existence of Tertiary plateau lavas
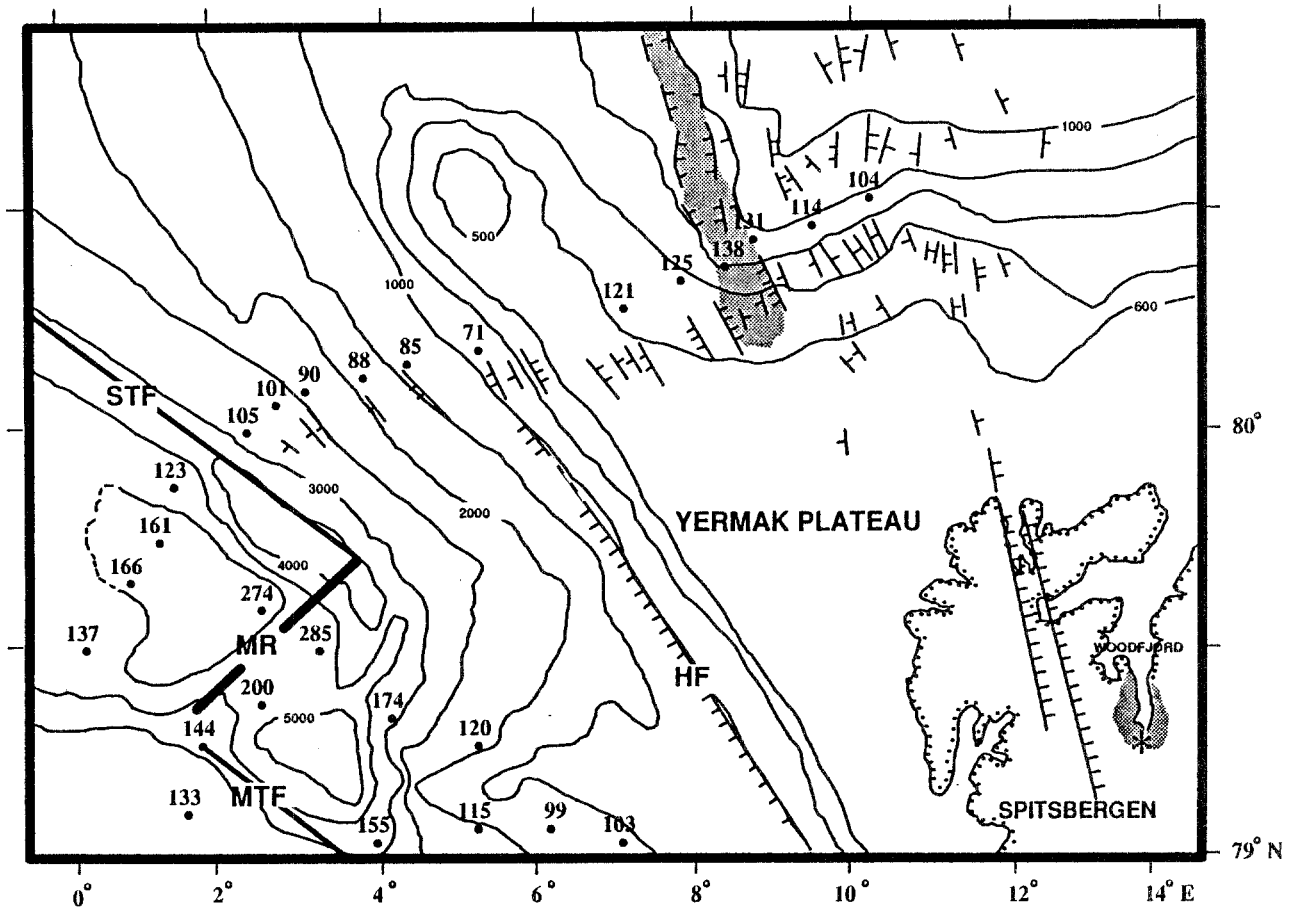

Fig. 4. Morphology and structures: the distribution of normal faults (interpreted from seismic cross sections collected by Sundvor *et al.*, 1982b) on the northwestern corner of Svalbard and the central Yermak Plateau. Locations of heat flow values – in milliwatts per square meter (dots), (from Crane *et al.*, 1982). The basement of the plateau is broken by numerous normal faults indicating a large complex graben system. Faults that define the NW-SE trending Woodfjord plateau basalts (stars) roughly lie in alignment with the western flank of the Yermak Plateau. Hornsund Fault (HF) lies along the western edge of the Plateau's crest and is bordered by the Spitsbergen Transform Fault (STF), Molloy Ridge (MR) and Molloy Transform Fault (MTF). Simplified bathymetry from Jackson *et al.* (1984) and Cherkis *et al.* (1991).

(Figure 4) in northern Spitsbergen (Prestvik, 1977). This obvious distinction between the northern and southern plateau suggests a dual origin for the plateau.

The central and southern plateau is topographically irregular and is broken by numerous normal faults (Sundvor et al., 1982b; Amundsen, 1988; Okay and Crane, 1990) that are thought to extend to the northern margin of Svalbard (Figure 4). There, Cenozoic volcanic centers are aligned along the normal faults which comprise the Woodfjord region (Skjelvale et al., 1989). Many of the major faults on the eastern margin of the plateau are the loci of high magnetic anomalies. One particular feature, the Mosby Peak, is marked by a distinct magnetic anomaly (250 nT) (Figure 3), and is located on the same set of faults which extend to the Woodfjord (Okay et al., 1991).

Heat Flow

Twenty four heat flow measurements (Crane et al., 1982; Jackson et al., 1984; Sundvor, 1986; Crane et al., 1991) were collected on the Yermak Plateau and surrounding areas (Figure 2). High heat flow values ($104-343$ mW m^2) are located on the southeastern Yermak Plateau aligned in a zone trending NNW-SSE from $80°$ N towards the coast of Svalbard (Figures 3 and 4). In contrast, heat flow on the northern plateau is lower with values in the range of $50-92$ mW m^{-2} (Jackson et al., 1984; Crane et al., 1982; Sundvor, 1986).

In the region of the high heat flow values, Sundvor et al. (1978, 1979, 1982a, 1982b) and Sundvor (1986) detected a near surface basement reflector (Figure 5), which they interpreted as a volcanic constructional feature which has overprinted continental crust. In some places the reflector is highly faulted. It has been found in most of the surveyed area disappearing under thick low velocity sediments towards the west and east (<2.5 km s^{-1}). On the basis of all available seismic data, Sundvor and Austegard (1990) have established this as a tentative oceanic-continental-crustal boundary, and is consistent with the plate reconstruction presented by Jackson et al. (1984) and Reksnes and Vågnes (1985).

Locating high heat flow on supposedly thinned continental crust suggests that some sort of intrusive activity exists on the Yermak Plateau and that it has undergone and is undergoing thermal rejuvenation. This interpretation is supported by the proximity of the plateau and this region of high heat flow with

Quaternary volcanism and hot springs (Amundsen et al., 1988; Skjelkvåle et al., 1989) in the Woodfjord area on Svalbard (Figures 3 and 4).

Crane et al. (1982) suggested that intrusive activity commenced 16 Ma and is continuing to the present. They also inferred that much of the relief of the plateau could be attributed to uplift by thrusting of intruded continental crust as a consequence of the propagation of the mid-ocean ridge further into the Spitsbergen Shear Zone. Bonatti and Michael (1989) concluded, after sampling fresh periodites from the Yermak Plateau's southern margin that the entire margin of Svalbard and the Yermak Plateau had been underplated, thinned and heated by mantle material associated with oceanic rather than continental mantle material.

The additional heat flow data presented by Sundvor (1986) provide us with a more complete set of thermal data in this area. Because of the structural complexity of the plateau, we use these heat flow data to test whether or not the plateau is undergoing breakup and rifting in the 'classical rifting' – cooling plate scenario or if it is undergoing asymmetric simple shear extension along faults that once were a part of the ancient Spitsbergen Shear Zone.

In the following sections we compare measured heat flow with that predicted by the cooling plate and the pure and simple shear models (Buck et al., 1988; Crane et al., 1991) to best determine the style of thermal rejuvenation on the Yermak Plateau.

Cooling Plate Modeling

During the cooling plate modeling process, different durations and initial times of heating were assumed. Crane et al. (1988) suggested that rifting began adjacent to central Svalbard between $35-40$ Ma. Therefore we used 40 Ma as the maximum onset age for intrusion into the Yermak Plateau. Additional evidence that this region has undergone more recent volcanism comes from the fact that Woodfjord ~ 100 km to the SE of our high heat flow readings has been subjected to Cenozoic volcanism that was initiated ~ 11 Ma and has probably continued into the Quaternary (Amundsen et al., 1988).

To accurately assess the heat flow on the plateau, the observed values have to be corrected for the blanketing effect due to sedimentation. Decompacted sediment thickness is calculated for each time of onset and dur-
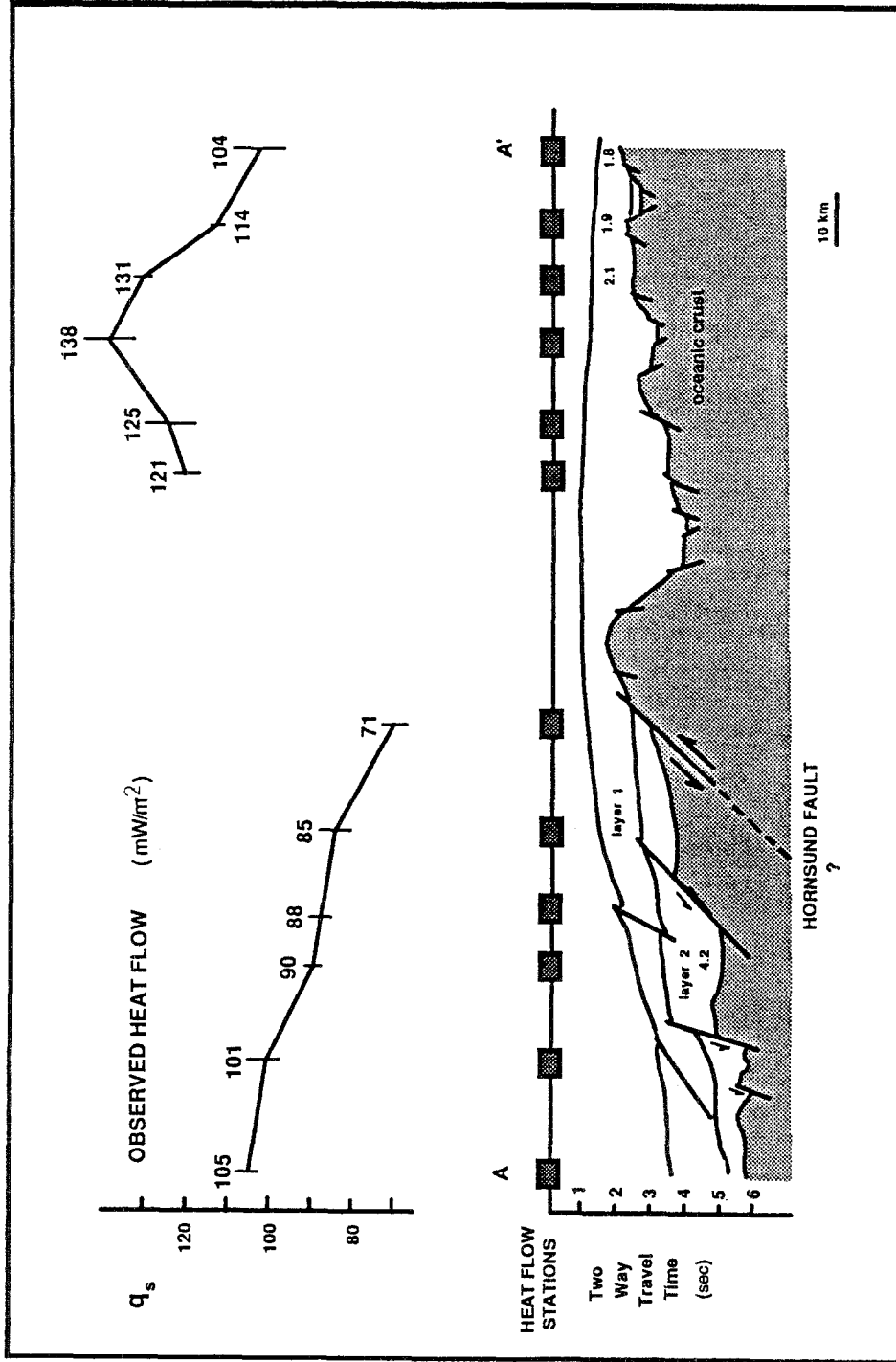
Fig. 5. Line drawing of a seismic cross section at 80° N collected by Sundvor *et al.* (1982) with observed heat flow (q$_s$) superimposed. Dark solid lines indicate interface between layer 1 and layer 2. Sediment seismic velocities (km/s) from sunobuoy refraction measurements along the line are indicated. The basement-reflector correlates with a 5.5 km s^{-1} refraction velocity. Depths to subsurface are estimated in seconds of two-way travel time. Numerous normal faults are indicative of stretched and extended crust. At the central Yermak Plateau, the acting Hornsund Fault buried under ice and thick low velocity sediments is determined to be a tentative ocean/continent boundary.

TABLE I

To compare observed surface heat flow (q_s) and corrected heat flow (q_b) the decompacted sediment thickness (H_{decomp}), porosities (ϕ), conductivities (K), specific heat of fluid (ρ_c), and diffusivities (κ) are computed. Depth (indicated by sec) and sediment thickness (H_{comp}) are calculated from two way travel time (TWT) and sediment seismic velocities at each heat flow station (St #)

					Layer 1				
Heat flow St #	Sediment seismic velocity (km s^{-1})	Depth z = TWT/2 (sec)	H_{comp} (km)	H_{decomp} (km)	Observed heat flow q_s (mW m^{-2})	$\phi(z)$	K	ρ_c ($\times 10^6$)	κ ($\times 10^7$ km my^{-1})
64	1.80	0.33	0.59	0.68	104	0.424	1.333	3.336	12.56
65	1.97	0.43	0.85	1.01	114	0.403	1.373	3.305	13.07
66	2.10	0.52	1.09	1.34	131	0.386	1.405	3.279	13.48
67	2.10	0.90	1.89	2.57	138	0.319	1.542	3.179	15.27
68	2.10	1.14	2.39	3.43	125	0.283	1.621	3.125	16.34
16	2.10	1.24	2.60	3.80	121	0.269	1.653	3.104	16.78

ation, sedimentation rates are estimated using two-way travel times and sediment seismic velocities derived from reflection, and refraction surveys in the area (Table I). If the heat flow from depth has been constant and if the sedimentation rate has been uniform, then the heat flow at the surface of the sediments can be estimated using an equation derived by Benfield (1949). Heat flow at each site is recomputed to predict what it should be both at the base

and the top of the sedimentary pile if the onset age and duration of heating are correct. The better fit of predicted with observed data is assumed to yield the most reasonable onset age and duration of heating.

Using the Hutchinson Model (Hutchinson, 1985) we calculated what the surface heat flow should be (predicted HF) for each station assuming that extension has taken place due to intrusive events lasting a fixed period of time (Table II). In addition, we used

TABLE II

For each episode, assuming various durations (my), calculated heat flow (q_b) and total rifting velocities (cm yr^{-1}) are determined. Distance to each heat flow station from the point of origin is shown. Sedimentation rate (sediment velocity in meters/million years) and corrected heat flow (q_b) values are calculated from the model for certain separation rates and sedimentation rates. RF (reduction factor) is the factor by which the heat flow is reduced. The difference between observed and calculated heat flow values is Δq, the mean $\Delta \bar{q}$, age, age of the crust (my) and average sedimentation rate (m/my) are given for each episode

Episode 1: 0–40 my
0.2 cm yr^{-1}

St #	Distance (km)	H_{decomp} (m)	Age (my)	Sed. rate (m my^{-1})	RF	q_s	q_b	Δq
64	23.10	680	22.9	29.7	1.048	104	109	5
65	13.99	1010	13.8	72.9	1.096	114	125	11
66	6.97	1340	6.9	194.2	1.168	131	153	22
67	0.96	2570	1.0	2570.0	2.232	138	308	170
68	10.82	3430	10.7	320.0	1.352	125	169	44
16	17.31	3800	17.1	221.8	1.273	121	154	33

Ave. sed. rate = 568.00 m my^{-1} $\Delta \bar{q}$ = 47.5 mW m^{-2}

Episode 2: 0–35 my
0.23 cm yr^{-1}

St #	Distance (km)	H_{decomp} (m)	Age (my)	Sed. rate (m my^{-1})	RF	q_s	q_b	Δq
64	23.10	680	20.01	33.99	0.034	104	109	5
65	13.99	1010	12.12	83.35	0.083	114	125	11
66	6.97	1340	6.04	221.97	0.222	131	155	22
67	0.96	2570	0.83	3090.88	3.091	138	335	170
68	10.82	3430	9.37	366.00	0.366	125	172	44
16	17.31	3800	14.99	253.46	0.254	121	159	33

Ave. sed. rate = 675.00 m my^{-1} $\Delta \bar{q}$ = 53.7 mW m^{-2}

TABLE II (*continued*)

Episode 3: 10–40 my
0.26 cm yr^{-1}

St#	Distance (km)	H$_{decomp}$ (m)	Age (my)	Duration (my)	Sed. rate (m my^{-1})	RF	q$_s$	q$_b$	Δq
64	23.10	680	17.8	27.8	24.5	1.121	104	109	5
65	13.99	1010	10.8	20.8	48.6	1.171	114	122	8
66	6.97	1340	5.4	15.4	87.0	1.147	131	147	16
67	0.96	2570	0.7	10.7	240.2	1.260	138	174	36
68	10.82	3430	8.3	18.3	187.4	1.259	125	157	32
16	17.31	3800	13.3	23.3	163.1	1.259	121	1592	31

Ave. sed. rate = 125.0 m my^{-1} Δq̄ = 21.3 mW m^{-2}

Episode 4: 10–35 my
0.32 cm yr^{-1}

St#	Distance (km)	H$_{decomp}$ (m)	Age (my)	Duration (my)	Sed. rate (m my)	RF	q$_s$	q$_b$	Δq
64	23.10	680	14.44	24.44	27.82	1.047	104	109	5
65	13.99	1010	8.74	18.74	53.90	1.076	114	125	9
66	6.97	1340	4.40	14.40	93.90	1.113	131	155	15
67	0.96	2570	0.60	10.60	242.45	1.261	138	335	36
68	10.82	3430	6.76	16.76	204.65	1.259	125	172	32
16	17.31	3800	10.83	20.83	182.43	1.259	121	159	31

Ave. sed. rate = 134.0 m my^{-1} Δq̄ = 21.3 mW m^{-2}

Episode 5: 11.5–40 my
0.28 cm yr^{-1}

St#	Distance (km)	H$_{decomp}$ (m)	Age (my)	Duration (my)	Sed. rate (m my^{-1})	RF	q$_s$	q$_b$	Δq
64	23.10	680	16.27	27.77	24.49	1.041	104	108	4
65	13.99	1010	9.85	21.35	47.30	1.071	114	122	9
66	6.97	1340	4.90	16.40	81.70	1.113	131	146	15
67	0.96	2570	0.68	12.18	211.07	1.230	138	170	32
68	10.82	3430	6.76	19.12	179.40	1.259	125	157	32
16	17.31	3800	12.20	23.70	160.40	1.259	121	152	31

Ave. sed. rate = 117.0 m my^{-1} Δq̄ = 20.3 mW m^{-2}

Episode 6: 11.5–35 my
0.34 cm yr^{-1}

St#	Distance (km)	H$_{decomp}$ (m)	Age (my)	Duration (my)	Sed. rate (m my^{-1})	RF	q$_s$	q$_b$	Δq
64	23.10	680	13.43	24.93	27.27	1.048	104	109	5
65	13.99	1010	8.14	19.64	51.44	1.070	114	122	8
66	6.97	1340	4.05	15.55	86.16	1.122	131	147	16
67	0.96	2570	0.56	12.06	213.10	1.229	138	170	31
68	10.82	3430	6.29	17.79	192.80	1.259	125	157	32
16	17.31	3800	10.07	21.57	176.20	1.259	121	152	31

Ave. sed. rate = 125.0 m my^{-1} Δq̄ = 20.3 mW m^{-2}

Episode 7: 18–35 my
0.5 cm yr^{-1}

ST#	Distance (km)	H$_{decomp}$ (m)	Age (my)	Duration (my)	Sed. rate (m my^{-1})	RF	q$_s$	q$_b$	Δq
64	23.10	680	9.72	26.72	27.82	1.047	104	108	4
65	13.99	1010	5.89	22.89	53.90	1.076	114	122	8
66	6.97	1340	2.93	19.93	93.06	1.113	131	144	13
67	0.96	2570	0.40	17.40	242.45	1.261	138	165	27
68	10.82	3430	4.55	17.70	204.65	1.259	125	154	29
16	17.31	3800	7.28	21.57	182.43	1.259	121	149	28

Ave. sed. rate = 134.0 m my^{-1} Δq̄ = 18.2 mW m^{-2}

a sedimentation rate calculated by knowing the de-compacted sediment thickness and the modeled age of the crust below. By comparing the predicted surface heat flow with the observed, we can estimate the extension rate across the Yermak Plateau and can predict the duration of the intrusion/s responsible for the stretching and extension of the plateau.

Results

We used seven different episodes for magmatic injection from 0 to 40 Ma testing the results of each

with our observed heat flow values. Two of the episodes assume that magmatic intrusion has continued to the present while five of the episodes assume that intrusion ceased between 10 and 18 Ma. Based on the amount of extension, determined by Jackson *et al.* (1984), and the width over which the heat flow anomalies occur, we varied the full rifting-separation rates from 0.2–0.5 cm yr^{-1}. The corrected values can be compared to those predicted by lithospheric cooling models (Parsons and Sclater, 1977; Hutchinson, 1985) (Table III; Figure 6).

TABLE III

Results from the oceanic cooling plate model. Corrected heat flow (q_b) compared to theoretical heat flow values (q_{s-p}) are determined from the age dependent cooling of the oceanic crust (McKenzie, 1978). The duration and age of the crust for each heat flow station at the ocean/continent boundary is corrected for sediment loading and shown. ΔHF is the difference between observed heat flow (q_b) and the cooling model-theoretical heat flow (q_{s-p}). The mean ($\overline{\Delta HF}$) values represent the goodness of fit. The possibility of a more ideal cooling history of the Plateau, Episode 4, gives a period of 10–35 my as the best fit, with a calculated $\overline{\Delta HF}$ value of 24.3 mW m^{-2} in a full separation rate (rifting velocity) of 0.32 cm/yr

| St # | *Episode 1* (0–40 my) | | | | *Episode 2* (0–35 my) | | | |
	Age (my)	q_b	q_{s-p}	ΔHF	Age (my)	q_b	q_{s-p}	ΔHF
64	22.9	109	100	9	20.1	109	111	2
65	13.8	125	130	5	12.12	125	140	15
66	6.9	153	188	35	6.04	155	189	34
67	1.0	308	840	532	0.83	335	950	615
68	10.7	169	150	19	9.37	172	160	12
16	17.1	154	120	39	14.99	159	128	31
		$\overline{\Delta HF} = 107$ mW m^{-2}				$\overline{\Delta HF} = 118$ mW m^{-2}		

| St # | *Episode 3* (10–40 my) | | | | *Episode 4* (10–35 my) | | | |
	Duration (my)	q_b	q_{s-p}	ΔHF	Duration (my)	q_b	q_{s-p}	ΔHF
	27.8	109	90	19	24.44	109	100	5
	20.8	122	108	14	18.74	123	115	9
	15.4	147	125	22	14.40	146	125	15
	10.7	174	150	24	10.60	174	150	36
	18.3	157	112	45	16.76	157	120	32
	23.3	152	100	52	20.83	152	105	31
		$\overline{\Delta HF} = 29.4$ mW m^{-2}				$\overline{\Delta HF} = 24.3$ mW m^{-2}		

| St # | *Episode 5* (11.5–40 my) | | | | *Episode 6* (11.5–35 my) | | | |
	Duration (my)	q_b	q_{s-p}	ΔHF	Duration (my)	q_b	q_{s-p}	ΔHF
	27.77	18	90	18	24.93	109	99	10
	21.35	122	105	17	19.64	122	111	11
	16.40	146	120	26	15.55	147	120	27
	12.18	170	140	30	12.06	169	140	30
	19.12	157	110	47	17.79	157	117	40
	23.70	152	100	52	21.57	152	110	42
		$\overline{\Delta HF} = 31.7$ mW m^{-2}				$\overline{\Delta HF} = 26.6$ mW m^{-2}		

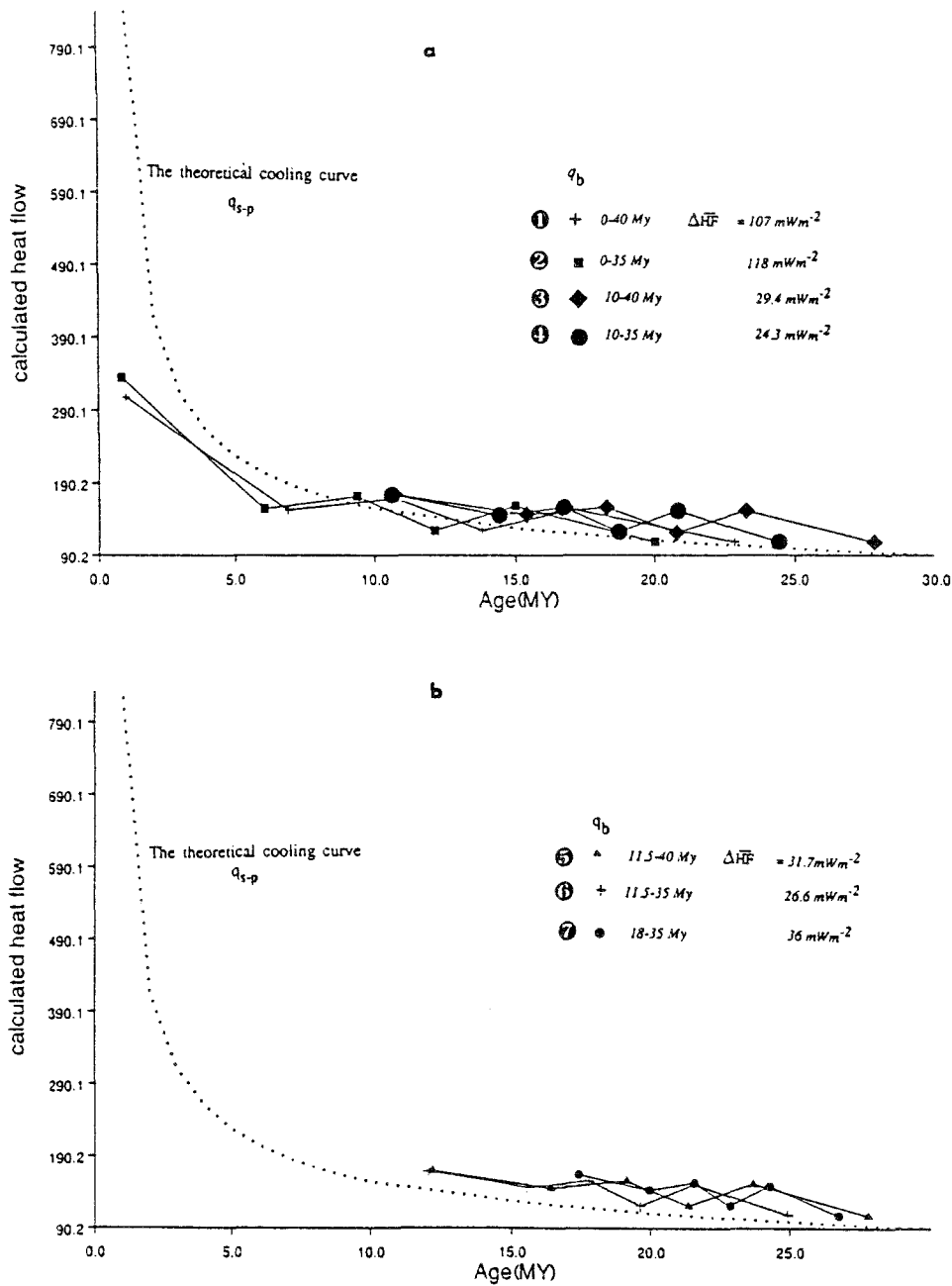| St # | *Episode 7* (18–35 my) | | | |
	Duration (my)	q_b	q_{s-p}	ΔHF
64	26.72	108	93	15
65	22.89	122	100	22
66	19.93	144	·110	34
67	17.40	165	120	45
68	21.55	154	105	49
16	24.28	149	97	52
	$\overline{\Delta HF} = 36$ mW m^{-2}			

Fig. 6. Corrected heat flow (q_b) across the central Yermak Plateau compared to predicted heat flow (q_{s-p}) from the McKenzie (1978) cooling plate model (dotted line) was adapted from Sclater and Parsons (1977). The seven episodes are represented in (a, b). Mean values ($\overline{\Delta HF}$) represent the goodness of fit. Note the best fit between the calculated heat flow and the cooling plate model: Episode 4's duration of 25 million years and the full separation rate of 0.32 cm yr^{-1}. (a) Station details are in Table III.

Although none of the episodes fits extremely well, the best fit between the models and the observed data suggest that magma began to intrude the Yermak Plateau ~35 Ma. At the same time transtension commenced along the Hornsund Fault (Müller and Spielhagen, 1990; Faleide *et al.*, 1991) and continued for 25 Ma, ceasing activity at 10 Ma. In this 'best fit'

episode, the average misfit ($\overline{\Delta HF}$) between the predicted and observed heat flow is ~24 mW m^{-2} compared to the worst fitting episode of a $\overline{\Delta HF}$ of 118 mW m^{-2} (for ongoing intrusion from 35 Ma to the present) (Figure 6). The results coincide nicely with the episode of volcanism at 11 Ma adjacent to the Woodfjord area. Figure 7 depicts the relative

Fig. 7. Thermal rejuvenation on the Yermak Plateau: the ocean/continent boundary age contours (bold) are drawn from the results of Episode 4, the best fit for the cooling plate model. The age of the crust (in my) for each heat flow station (dot) is shown in Table II. These results coincide with the Quarternary volcanic eruptions, particularly the Woodfjord plateau basalts (star) estimated at between 10 and 15 million years. Simplified bathymetry (m) adapted from Jackson *et al.* (1984) and Cherkis *et al.* (1991).

ages of intrusion and extension on the Yermak Plateau assuming that the cooling plate model adequately represents the intrusive activity in this region.

Pure and Simple Shear Numerical Modeling

Because there is a very high probability that much of the Yermak Plateau is still continental crust, the oceanic cooling plate model is probably not adequate. It may be more appropriate to model the thermal evolution of thinning and extending continental crust under both simple as well as pure shear conditions (Buck et al., 1988; Crane et al., 1991).

The direct observations of normal faults extending to great depths in the continental crust combined with observations of topographic asymmetries across many young rifts have led to the suggestion that normal faults and/or ductile shear zones may extend through the lithosphere (Wernicke, 1985). The lithospheric detachment model indicates that much of the deformation in an extending region occurs as simple shear extension rather than pure shear.

The rifting geometries we consider are both simple shear extension along planar lithospheric detachment faults, and pure shear extension within a zone that can change its width over time. Pure and simple shear extension of the lithosphere can produce very different patterns of heat flow, structure and topography within a rift and the neighboring young continental margins (Figure 8). The pure shear model of extension can be produced by using a high plate separation rate or a narrow zone of pure shear extension, where melting is centered symmetrically underneath (McKenzie, 1978).

In contrast, listric fault geometry will be produced by a single simple shear detachment if there is a finite width of isostatic response. Lower plate crust is progressively stripped off the center of the simple shear rift, but at no point is the advected lithosphere near the mantle solidus (Buck et al., 1988). With continued extension, the lithosphere eventually generates a steady-state temperature structure which is homogeneous everywhere below the mantle solidus. The total amount of opening rate and also the angle of the detachment dip determine the total heat input onto the lithosphere and how much time and how much of the original heat input from the asthenosphere remains for a particular geometry of extension.

Results

In Figures 9a and 9b, each 'time-dependent model' portrays different results for crustal thinning, heat flow, thermal uplift and subsidence assuming an initial rift width and a given plate separation rate. The model results are dependent on only the temperature structure of the model lithosphere and the distribution of the crustal thickness. Symmetric pure shear extension cannot match the predicted heat flow and topography with the observed across the Yermak Plateau (Figure 9a). Very slow spreading rates cannot produce conditions approaching the mantle solidus anywhere in the lithosphere. In addition, simple shear across a shallow (22°) dipping detachment fault does not match the observed heat flow nor is the topography of the Yermak Plateau anywhere reproduced by the model (Figure 9b).

Simple shear extension along a steeply dipping detachment fault has been proposed by Crane et al. (1991) to explain the observed asymmetric topography across the Knipovich Ridge to the south of the Yermak Plateau. On the plateau itself, another system of normal faults oriented NW-SE extends from the high heat flow province into the volcanically active Woodfjord area located on the western side of Svalbard. Our best fit between the heat flow, the net topography and the structure on the plateau with the modeled results requires a detachment fault which cuts through the plateau dipping to the SW at an angle of at least 45° intersecting a deep seated Knipovich Ridge detachment surface (Figure 10). In this case, intrusion commenced at 35 Ma with extension and thinning of the crust (originally 30 km thick), continuing up to the present resulting in a full separation rate of $0.32\ cm\ yr^{-1}$. The modeled episode fits best with a broad zone of intrusion creating forty kilometers of structurally thinned and thermally rejuvenated continental crust.

An illustration representing the two intersecting detachment surfaces (Figure 11) shows our proposed structural model for the Yermak Plateau. In this case, the primary detachment fault dips eastwards underneath the Svalbard margin where it intersects the westward dipping detachment fault cutting through the Yermak Plateau. Both detachment surfaces could be inherited from the faults associated with the ancient Spitsbergen Shear Zone making them excellent conduits for the rise of magma to the
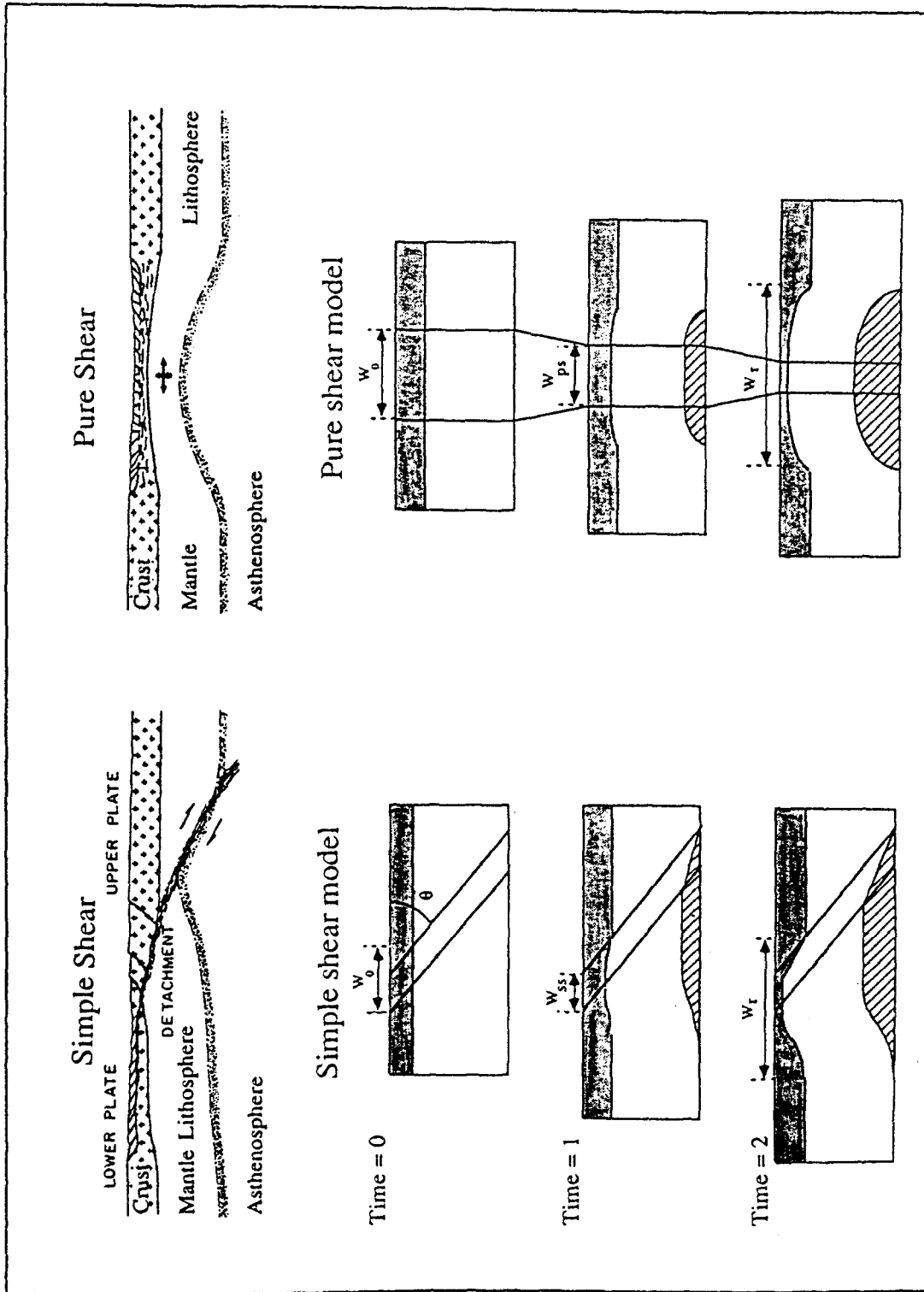
Fig. 8. Schematic cross-section of Lithosphere/Asthenosphere after rifting. A pure shear extension model produces a symmetrical cross-section of the deformed brittle upper layer of the lithosphere over a ductile lower layer. The simple shear extension moves along a continuous low-angle detachment. The detachment divides the lithosphere into an 'upper plate' and 'lower plate' or a hanging wall and footwall. Thinning of the lower lithosphere is offset along the detachment from the thinning of the upper lithosphere, producing an asymmetric lithospheric cross-section. Parameters are defined after Buck et al. (1988).

Topography

Heat Flow

Lithospheric Section
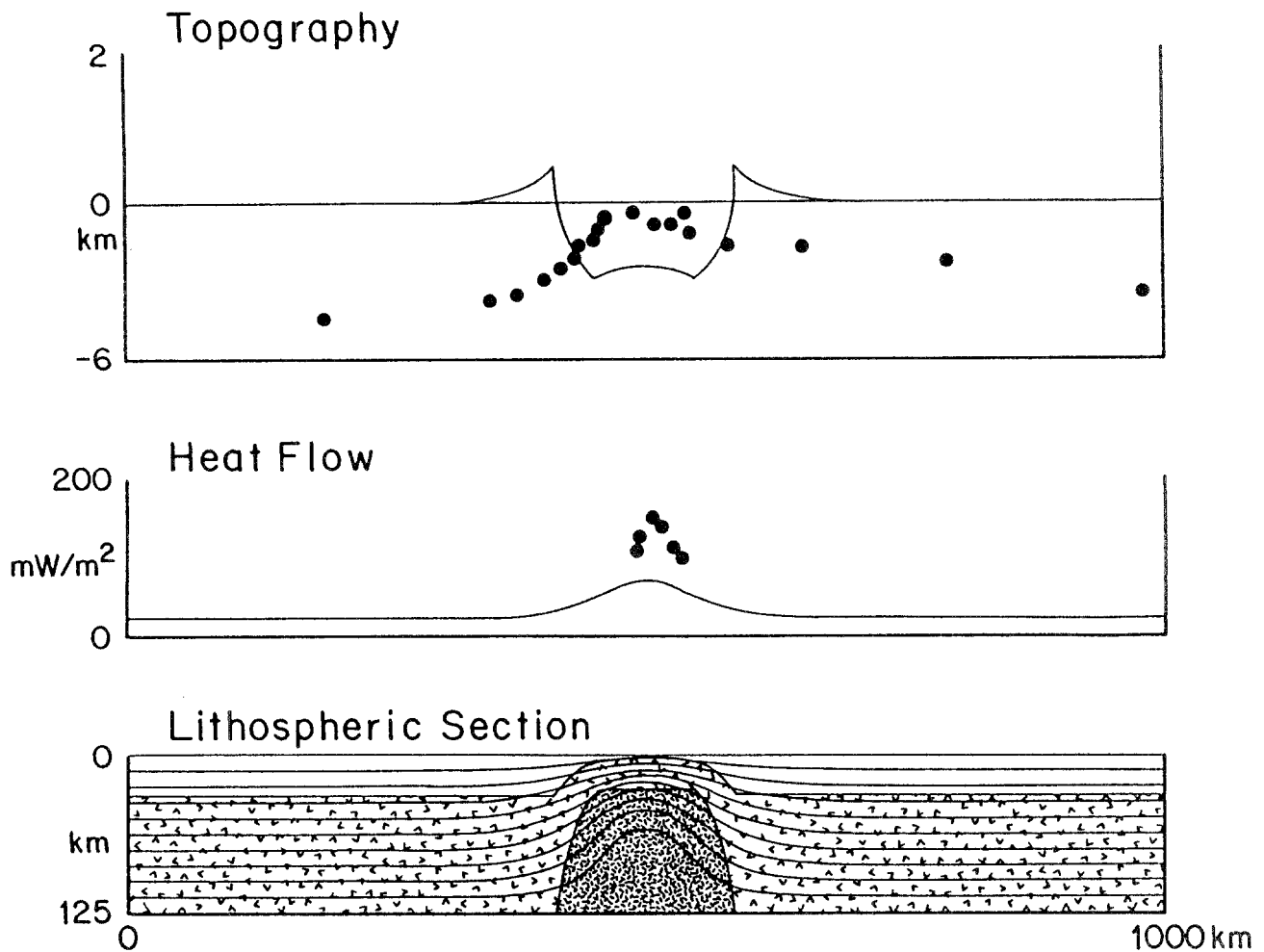
Fig. 9(a). The best fit (Episode 4) with pure shear extension evolved at 35 my in a full separation rate of about 0.32 cm y^{-1}; total present-day offset across the region is 112 km. The initial crustal thickness was 32 km (un-shaded region of the lithospheric section) and the initial rift width was 48 km. Observed sea-floor topography and heat flow are shown by dots. Heat flow stations are superimposed on the heat flow curve. Curvilinear lines in the lithospheric section show isotherms and dark shaded region that indicates an upwelling asthenosphere. Horizontal and vertical scales are in kilometers. Grid dimensions are 13 × 104.

surface, enabling the extrusion of basalt ten's of kilometers distant from the axis of the major detachment.

Conclusion

We propose that northwards propagation of the Mohns Ridge has allowed asthenospheric melt to erupt first out of the Knipovich Ridge, the major detachment surface. Further injection has probably occurred along secondary faults which have trapped upwelling magma at their points of intersection with the primary fault. In this case the minor extrusion occurred where the secondary fault cuts the surface along the Yermak Plateau.

Little direct evidence suggests that detachment faults cut through the Svalbard crust, primarily because nobody has looked deeply enough into the crust to say one way or the other. However, steeply dipping detachment surfaces could explain why the Svalbard archipelago is seismically active compared to the relatively quiet Boreas basin and Greenland margin. In addition, the tapping of magma from its source to a region underlying Svalbard could explain the tremendous rate of uplift that Svalbard has undergone during the last five million years. At the present, no other model better explains the extreme thermal, seismic and topographic asymmetries across the Norwegian-Greenland Sea.

Simple shear model. WO (km) = 25.0			Crustal thickness (km)	=	32.0
Time (M.Y.)	=	35.1	Angle (degrees)	=	22.0
Offset (km)	=	112.2	Velocity (cm/yr)	=	0.3
			Grid dimensions	=	13 x 100

Topography
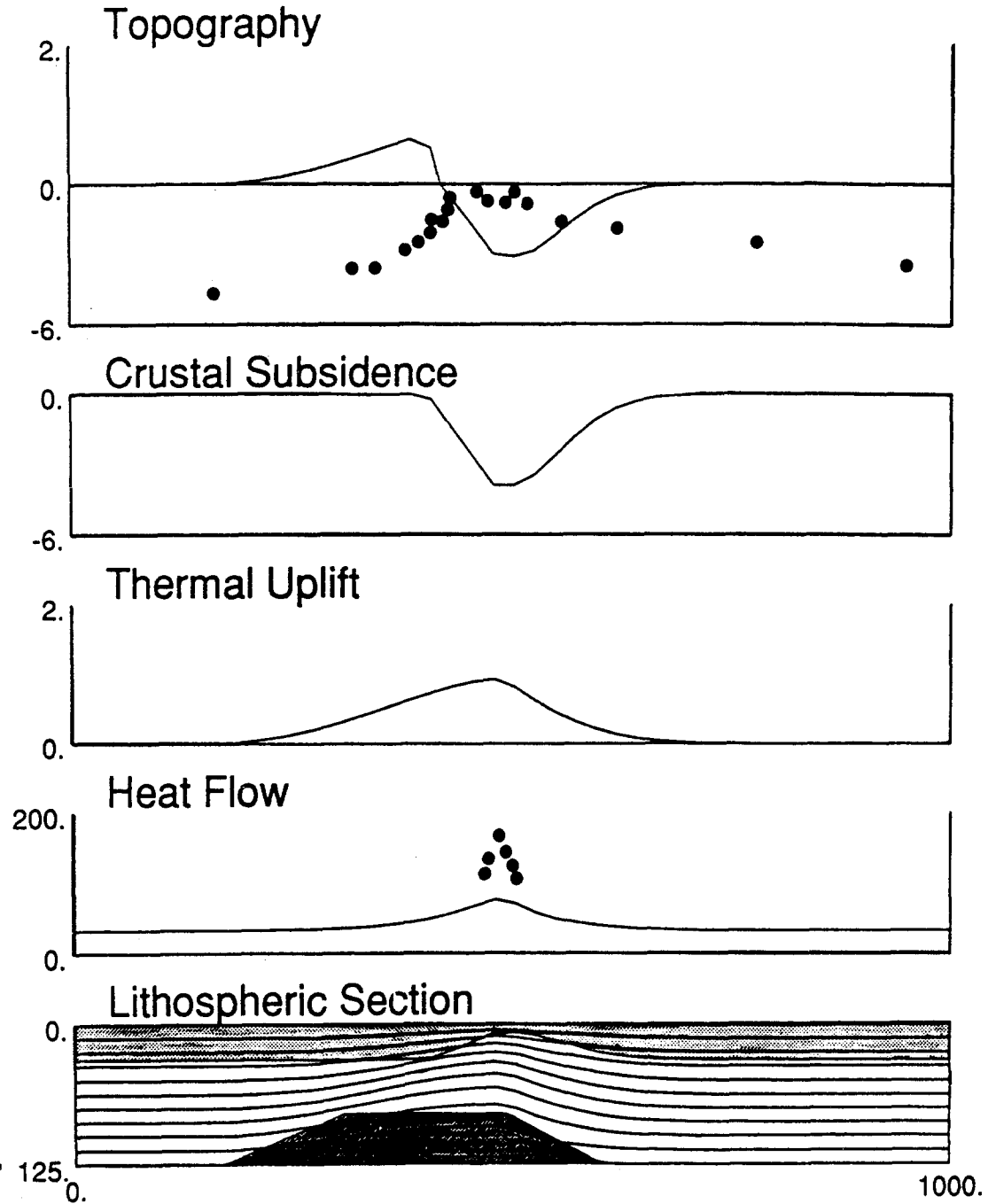
Crustal Subsidence

Thermal Uplift

Heat Flow

Lithospheric Section

Fig. 9(b). The best fit between simple shear that evolved to 35 my at a rifting velocity of about 0.32 cm yr^{-1}, along a low-angle (22°) detachment fault to the west of the Knipovich Ridge and corrected heat flow and seafloor topography values. Observed seafloor topography corrected for sediment loading (dots) is superimposed on the computed topography curve (in milliwatts per square meter) and is the sum of crustal subsidence and thermal uplift. In this case, initial crustal thickness was 32 km and the initial rift width was 25 km. Present-day offset across the rifted region is 112 km.

Topography

45°
0.8 cm/yr

47°
0.32 cm/yr

Crustal Subsidence

Thermal Uplift

Heat Flow

● YERMAK
  PLATEAU
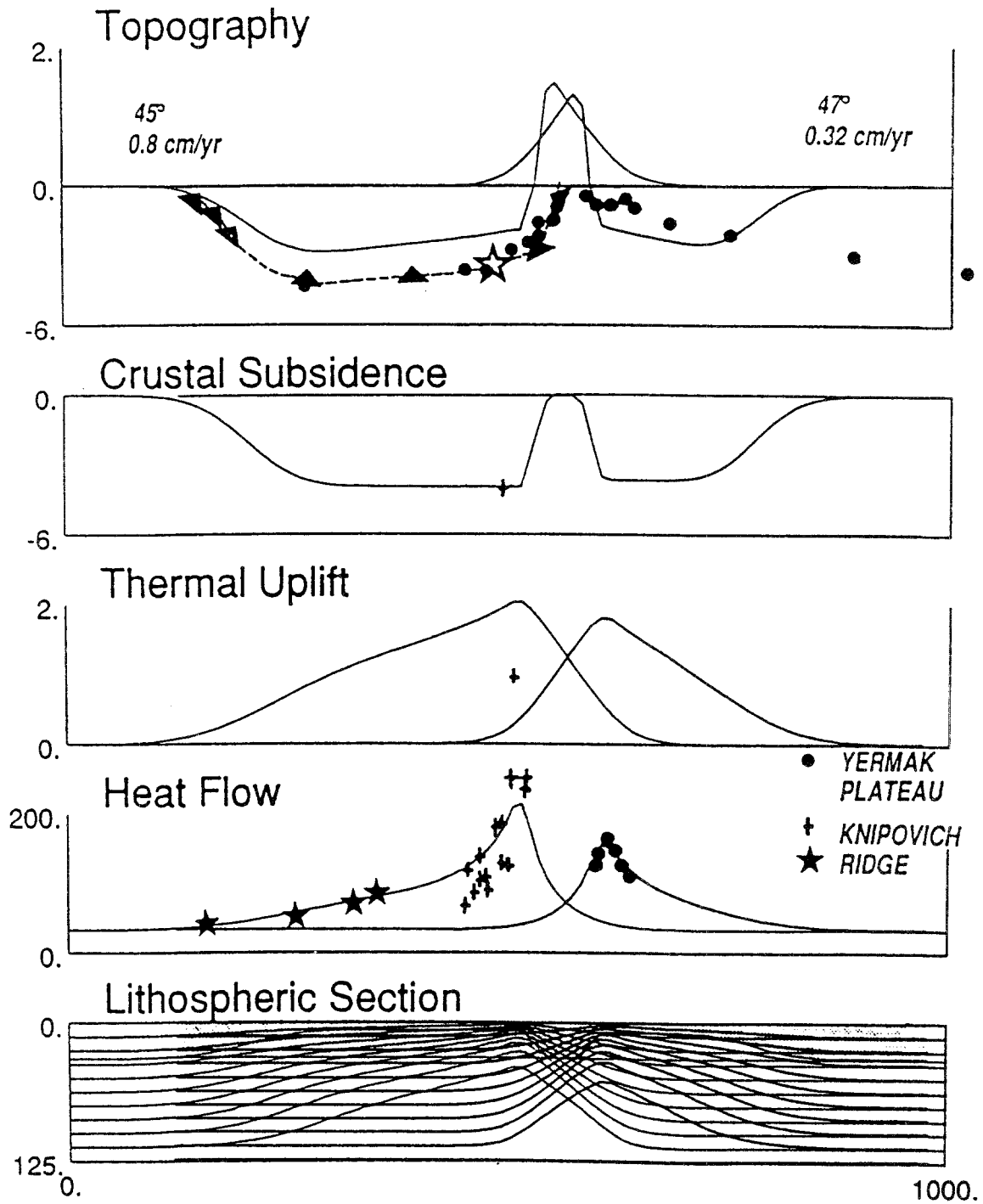
✝ KNIPOVICH
★ RIDGE

Lithospheric Section

Fig. 10. A complex shear model displacing two detachment faults (both 45°) dipping toward one another is proposed to explain the observed asymmetric topography and heat flow across the Knipovich Ridge to the south of the Yermak Plateau. The Knipovich Ridge axis (open star) is at 78° N. The initial crustal thickness for both models was 32 km at the initial point of rifting, and present-day offset across the ridge axis is 321 km.
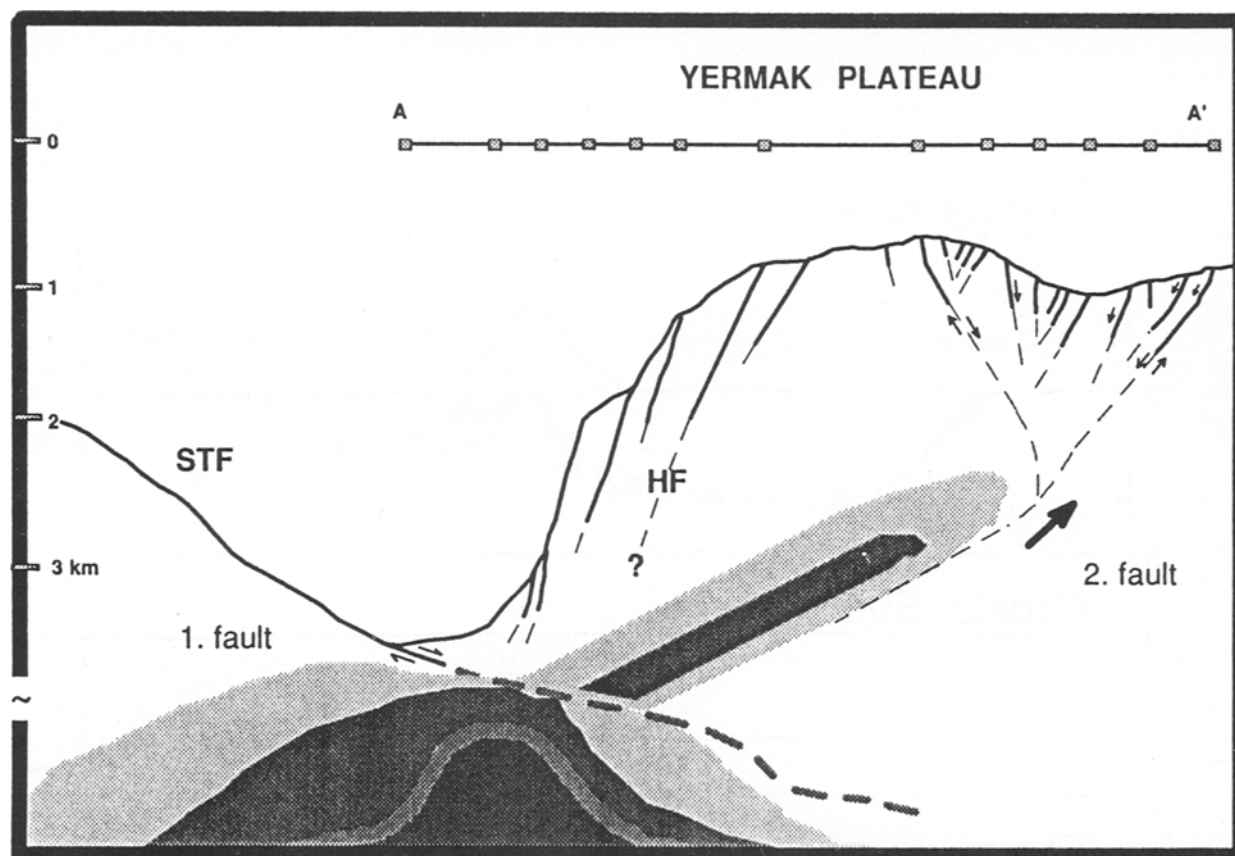
Fig. 11. Evolutionary structural model representing faults dipping eastwards from the Spitsbergen Transform Fault (STF)-Knipovich Ridge (underneath Svalbard) intersecting a secondary fault dipping westward. (AA') represents the same heat flow profile for the central Yermak Plateau on Figure 5. Magma upwelling under the Knipovich detachment is also tapped by the secondary fault which intersects the seafloor on the Yermak Plateau, leading to thermal rejuvenation of older continental crust.

Recent data collected by the SeaMARC II system (Sundvor *et al.*, 1991; Okay *et al.*, 1991) suggest that other faults parallel to and east of the Yermak Plateau have been the sites of massive outpourings of basalt. As no heat flow data exist in this region we are unable to make any age estimates of the intrusion dates. However, the data on the Yermak Plateau coupled with the recently active volcanism adjacent to the Woodfjord area, show that this region has undergone and is probably still undergoing fairly large scale thermal rejuvenation.

Acknowledgements

References

Amundsen, H. E. F., Griffin, W. L., and O'Reilly, S. Y., 1988, The Nature of the Lithosphere beneath Northwestern Spitsbergen: Xenolith Evidence, *Nor. geol. unders. Special Publ.* **3**, 58–65.

Benfield, A. E., 1949, The Effect of Uplift and Denudation on Underground Temperatures, *J. App. Phys.* **20**, 66–70.

Birkenmajer, K., 1981, The Geology of Svalbard, the Western Part of the Barents Sea, and the Continental Margin of Scandinavia, in: A. E. Nairn, M. Churkin, and F. G. Stehli (Eds), *The Ocean Basins and Margins, The Arctic Ocean*, Plenum Press, New York, vol. 5, pp. 265–330.

Bonatti, E., 1985, Punctiform Initiation of Seafloor Spreading in the Red Sea During the Transition from a Continental to an Oceanic Rift, Nature 316, 33–37.

Bonatti, E. and Michael, P. J., 1989, Mantle Peridotites from Continental Rifts, to Ocean Basins to Subduction Zones, Earth Planet. Sci. Lett. 91, 297–311.

Bonatti, E. and Crane, K., 1984, The Geology of Oceanic Transform Faults, Scientific American 250, (5), 40–51.

Bonatti, E. and Crane, K., 1982, Oscillatory Spreading Explanation of Anomalously Old Uplifted Crust near Oceanic Transforms, Nature 300, 343–345.

Buck, W. R., Martínez, F., Steckler, M. S., and Cochran, J. R., 1988, Thermal Consequences of Lithospheric Extension: Pure and Simple, Tectonics 7, 213–234.

Cherkis, N. Z., Fleming, H. S., Max, M. D., and Vogt, P. R., 1991, Bathymetry Map of the Barents and Kara Seas, U.S. Naval Res. Lab.

Crane, K., Sundvor, E., Buck, R., and Martínez, F., 1991, Rifting in the Northern Norwegian-Greenland Sea: Thermal Tests of Asymmetric Spreading, J. Geophys. Res. 96, (B9), 14529–14550.

Crane, K., Sundvor, E., Foucher, J. P., Hobart, M., Myhre, A. M., and LeDouaran, S., 1988, Thermal Evolution of the Western Svalbard Margin, Marine Geophys. Res. 9, 165–194.

Crane, K. and Bonatti, E., 1987, Fracture Zone Control on the Opening of the Red Sea: SIR A Data, J. Geol. Soc. London 144, 407–420.

Crane, K., Eldholm, O., Myhre, A. M., and Sundvor, E., 1982, Thermal Implications for the Evolution of the Spitsbergen Transform Fault, Tectonophysics 89, 1–32.

Courtillot, V., 1982, Propagating Rifts and Continental Breakup, Tectonics 1, 239–250.

Dietz, R. S. and Shumway, G., 1961, Arctic Basin Geomorphology, Bull. Geol. Soc. Am. 72, 1310–1330.

Faleide, J. I., Gudlaugsson, S. T., Eldholm, O., Myhre, A. M., and Jackson, H. S., 1991, Deep Seismic Transects across the Sheared Western Barents Sea-Svalbard Continental Margin, Tectonophysics 189, 73–89.

Feden, R. H., Vogt, P. R., and Fleming, H. S., 1979, Magnetic and Bathymetric Evidence for the 'Yermak' Hot Spot Northwest of Svalbard in the Arctic Ocean, Earth Planet Sci. Lett. 4, 18–38.

Hutchinson, I., 1985, The Effects of Sedimentation and Compaction on Oceanic Heat Flow, Geophys. J. R. Astr. Soc. 82, 439–459.

Jackson, H. R., Johnson, G. L., Sundvor, E., and Myhre, A. M., 1984, The Yermak Plateau: Formed at a Triple Junction, J. Geophys. Res. 89 (B5), 3223–3232.

Johnson, G. L., 1975, Morphology and Structure of the Norwegian-Greenland Sea, Dissertation, Univ. Copenhagen, 157 pp.

Lister, G. S., Etheredge, M. A., and Symonds, P. A., 1986, Detachment Faulting and the Evolution of Passive Continental Margins, Geology 14, 246–250.

Martínez, F. and Cochran, J. R., 1988, Structure and Tectonics of the Northern Red Sea: a Continental Margin between Rifting and Drifting, Tectonophysics 150, 1–32.

McKenzie, D. P., 1978, Some Remarks on the Development of Sedimentary Basins, Earth Planet. Sci. Lett. 40, 25–32.

Müller, R. D. and Spielhagen, R. J., 1990, Evolution of the Central Tertiary Basin of Spitsbergen: towards a Synthesis of Sediment and Plate Tectonic History, Paleogeography, Paleoclimatology, Paleoecology 80, 153–172.

Myhre, A. M. and Eldholm, O., 1988, The Western Svalbard Margin (74–80), Marine Petrol. Geol. 5, 134–156.

Okay, N., 1990, Thermal Modeling of the Yermak Plateau within the Norwegian-Greenland Sea, M.S. thesis, 117 pp, New York City Univ., New York.

Okay, N. and Crane, K., 1990, Thermal Modeling of the Yermak Plateau within the Norwegian-Greenland Sea, (Abs.) EOS Trans. 71, 17, 622.

Okay, N., Crane, K., Vogt, P. and Sundvor, E., 1991, Diffuse Rifting and Associated Volcanism on the Yermak Plateau in the Arctic Ocean: SeaMARC II results, Part IV. (Abs.) EOS Trans. 72, 17, 274.

Parsons, B. G. and Sclater, J., 1977, An Analysis of the Variation of Ocean Floor Heat Flow Bathymetry with Age. J. Geophys. Res. 82, 803–827.

Prestvik, T., 1977, Cenozoic Plateau Lavas of Spitsbergen – A Geochemical Study, Nor. Polarinst. Årb., p. 127–143.

Reksnes, P. A. and Vågnes, E., 1985, Evolution of the Greenland Sea and Eurasian Basin, M.S. thesis, 136 pp. Oslo Univ., Norway.

Skjelvåle, B., Amundsen, H. E. F., O'Reilly, S. Y., Griffin, W. L., and Gjelsvik, T., 1989, A Primitive Alkali Basalts Stratovolcano and Associated Eruptive Centers, Northwestern Spitsbergen: Volcanology and Tectonic Significance, J. Volcanol. Geotherm. Res. 37, 1–19.

Srivastava, S. P. and Roest, W. P., 1989, Seafloor Spreading History II–VI, in: J. S. Bell (coordinator), East Coast Basin Atlas Series: Labrador Sea. Atlantic Geosci. Cent. Geol. Surv. Can., Map sheet L17-2–L17-6.

Sundvor, E., 1986, Heat Flow Measurements on the Western Svalbard Margin, Univ. Bergen Seismol. Observ. Sci. Rep., 11 pp.

Sundvor, E., Crane, K., Vogt, P. R., Martínez, F., Jones, C., deMoustier, C., Doss, H., Okay, N., and SeaMARC Team (A. Shor, M. Rognstad, S. Dong, D. Johnson and D. Bergensen), 1991, SeaMARC II and Associated Geophysical Investigation of the Knipovich Ridge, Molloy Ridge/Fracture Zone and Barents/ Spitsbergen Continental Margin: Part I. Overview of Two Year Program Completed. (Abs.) EOS Trans. 72, 22, 232.

Sundvor, E. and Austegard, A., 1990, The Evolution of the Svalbard Margins: Synthesis and New Results, in U. Bleil and Thiede (eds.), Geological History of Polar Oceans: Arctic versus Antarctic, Kluwer Acad. Publ., Netherlands 77–94.

Sundvor, E., Myhre, A. M., Austegard, A., Haugland, K., Eldholm, O., and Gidskehang, A., 1982a, Marine Geophysical Survey on the Yermak Plateau, Univ. Bergen Seismol. Observ., Sci. Rep. 7, 26 pp.

Sundvor, E., Leonard, G. J., and Myhre, A., 1982b, Some Aspects of Morphology and Structure of the Yermak Plateau, Northwest of Spitsbergen, Univ. Bergen Seismol. Observ., Sci. Rep. 8, 29 pp.

Sundvor, E., Myhre, M. A., and Eldholm, O., 1979, The Svalbard Continental Margin, Norwegian Sea Symposium, Norw. Petrol. Soc. NSS/6, 1–25.

Sundvor, E., Gidskehang, A., Myhre, A. M., and Eldholm, O., 1978, Marine Geophysical Survey on the Northern Svalbard Margin, Univ. Bergen Seismol. Observ., Sci. Rep. 5, 46 pp.

Talwani, M. and Eldholm, O., 1977, Evolution of the Norwegian-Greenland Sea, Geol. Soc. Amer. Bull. 88, 969–999.

Thiede, J., Pfirman, Schenke, H.-W., and Reid, W., 1990, Bathymetry of Molloy Deep: Fram Strait between Svalbard and Greenland, Mar. Geophys. Res. 12, 197–214.

Vogt, P. R., Perry, R. K., Feden, R. H., Fleming, H. S., and Cherkis, N. Z., 1981, The Greenland-Norwegian Sea and Iceland environment: Geology and Geophysics, in: A. E. M. Nairn and M. Churkin (Eds), The Ocean Basins and Margins 5, 493–598.

Wernicke, B., 1985, Uniform-Sense Normal Simple Shear of the Continental Lithosphere, Can. J. Earth Sci. 22, 108–125.

Winsnes, T., 1965, The Precambrian of Spitsbergen and Bjørnoya, in: K. Rankama (Ed), The Geological Systems, The Precambrian, John Wiley, New York, vol. 2, pp. 1–24.